Precambrian Research 169 (2009) 15–27

Contents lists available at ScienceDirect

Precambrian Research

journal homepage: www.elsevier.com/locate/precamres

Isotopic constraints on the Late Archean carbon cycle from the Transvaal Supergroup along the western margin of the Kaapvaal Craton, South Africa

W.W. Fischer[a,*], S. Schroeder[b], J.P. Lacassie[b], N.J. Beukes[b], T. Goldberg[c], H. Strauss[d], U.E. Horstmann[e], D.P. Schrag[a], A.H. Knoll[a,f]

[a] Department of Earth and Planetary Sciences, Harvard University, Cambridge, MA, USA
[b] Department of Geology, University of Johannesburg, Johannesburg, South Africa
[c] School of Earth Sciences, James Cook University, Townsville, Australia
[d] Geologisch-Paläontologisches Institut, Westfälische Wilhelms-Universität Münster, Germany
[e] Environmental Isotope Group, iThemba Labs Gauteng, Wits, South Africa
[f] Department of Organismic and Evolutionary Biology, Harvard University, Cambridge, MA, USA

ARTICLE INFO

Article history:
Received 5 July 2007
Received in revised form 6 January 2009
Accepted 7 January 2009

Keywords:
Campbellrand
Iron formation
Microbialite
Iron respiration
Biological pump
Siderite

ABSTRACT

Few existing studies illuminate the operation of the carbon cycle before the rise of atmospheric oxygen circa 2400 million years ago. Stable carbon isotopic measurements of shallow stromatolitic carbonates (~0‰ VPDB) and basinal carbonate minerals (−6‰) in iron formation have been used to infer a strong isotopic depth gradient in Archean ocean basins. From new diamond drill cores obtained by the Agouron Drilling Project from the Griqualand West structural basin in the Northern Cape Province, South Africa, we present $\delta^{13}C$ data from carbonates and organic matter that offer fresh insights into the Late Archean carbon cycle. Three drill cores cover the development, progradation, and ultimate demise (by drowning) of the Campbellrand carbonate platform (ca. 2590–2500 Ma); one captures the platform top shallow marine and intertidal paleoenvironments, the other two run through slope and basinal sections deposited adjacent to the platform margin, increasing in water depth (likely to >1 km). Both shallow and deep-water carbonates precipitated on the seafloor consistently show $\delta^{13}C$ values around −0.5‰, incompatible with a strong Late Archean isotopic depth gradient. A mathematical model suggests that these isotopic data are consistent with a reduced biological pump, increased dissolved inorganic carbon in seawater due to higher atmospheric P_{CO2}, or both. Certain horizons do show distinct isotopic variability. Such areas are commonly shaly, and they tend to be organic and/or iron rich. Strong C-isotopic variations occur on a cm scale and most likely stem from diagenetic remineralization of organic matter. In sediment-starved areas where iron formation developed, siderite tends to be ^{13}C-depleted, sometimes by as much as −14‰. These observations suggest a carbon cycle in which iron respiration played a conspicuous role. Carbon isotope ratios from organic matter in shales are commonly >1‰ lighter than stratigraphically contiguous carbonates, but there is no clear water depth trend in the organic carbon isotopic data. Taken as a whole, the $\delta^{13}C$ of organic matter can be explained by several non-unique sets of processes, including different autotrophic mechanisms of carbon fixation, heterotrophic recycling (including fermentation and methanotrophy), and post-depositional diagenesis. The most striking feature is the occurrence of organic $\delta^{13}C$ values <−40‰, a feature that appears to be commonplace in Late Archean successions. Framed in the context of carbon cycle isotopic mass balance, both organic and carbonate carbon isotopic data suggest that the proportion of carbon buried as organic matter was not radically different before the appearance of free environmental oxygen.

1. Introduction

The initial rise of atmospheric O_2 constitutes one of the most biologically significant environmental transitions in Earth history, and derives, ultimately, from a biological innovation, the evolution of oxygenic photosynthesis. The fate of photosynthetic O_2 (rapid remineralization or accumulation in the oceans and atmosphere), however, is linked to the full range of carbon cycle processes via the burial flux of organic matter. Based on observations of carbon

Abbreviations: Ga, giga annum before present; Ma, mega annum before present; VPDB, Vienna Pee Dee belemnite standard; $\delta^{13}C$, $\delta^{13}C = ((^{13}R_{sample} - {}^{13}R_{std.})/{}^{13}R_{std.}) \times 1000$; ^{13}R, $^{13}R = {}^{13}C/{}^{12}C$; $\delta^{18}O$, $\delta^{18}O = ((^{18}R_{sample} - {}^{18}R_{std.})/{}^{18}R_{std.}) \times 1000$; ^{18}R, $^{18}R = {}^{18}O/{}^{16}O$.

* Corresponding author. Current address: Division of Geological and Planetary Sciences, California Institute of Technology, 1200 E. California Blvd., MC 170-25, Pasadena, CA 91125, USA. Tel.: +1 626 395 3417; fax: +1 626 568 0935.
E-mail address: wfischer@caltech.edu (W.W. Fischer).

0301-9268/$ – see front matter © 2009 Elsevier B.V. All rights reserved.
doi:10.1016/j.precamres.2008.10.010

isotopic data, previous work suggested that the Archean carbon cycle operated in a manner different from younger times in Earth history, with little or no burial of organic carbon. To test these hypotheses, we employed a combination of theory, new geologic observations, and new isotopic data, that enable us to assay critical processes in the Late Archean carbon cycle, just prior to the rise of environmental O_2.

The carbon cycle functions as a central hub that connects all biogeochemical cycles operating at the Earth's surface. Over sufficiently long time scales (>250 kyears) carbon emitted from the solid Earth has two well-known sedimentary sinks: organic matter and carbonate salts (Ebelmen, 1845). A large kinetic isotope fractionation occurs when carbon is fixed into organic matter (Nier and Gulbrandsen, 1939; Urey, 1947; Farquhar and Ehleringer, 1989). As a result, the stable carbon isotopic composition of organic matter and carbonates changes sympathetically with the proportional amounts of carbon removed to these two sinks. This is fortunate because rather than attempting to measure the absolute amount of carbonate and organic carbon buried over a given time interval (extremely challenging, given the strong preservational biases inherent to the geologic record), we can instead estimate the fraction of carbon buried as organic matter relative to total carbon burial by measuring the isotopic composition of both carbonates ($\delta^{13}C_{carb}$) and organic matter ($\delta^{13}C_{org}$) from selected, well-preserved stratigraphic successions (Wickman, 1956) (Eq. (1)):

$$f_{org} = \frac{\delta^{13}C_{carb} - \delta^{13}C_{input}}{\delta^{13}C_{carb} - \delta^{13}C_{org}} \quad (1)$$

This parameter, referred to here as f_{org}, represents the proximal interface between acid–base and reduction–oxidation processes occurring on the fluid Earth and offers a readily attainable measure of the state of the global carbon cycle at the geological instant of sedimentation.

The accumulation of oxidized species in the oceans and atmosphere ultimately derives from organic carbon that escapes remineralization by means of sedimentary burial (shifting the Eq. (2) equilibrium to the right):

$$CO_2 + H_2O \Leftrightarrow CH_2O + O_2 \quad (2)$$

Although few studies detail carbon cycle mechanics during Archean time, available data considered in the context of isotopic mass balance with known inputs (Schidlowski et al., 1975; Beukes et al., 1990; Strauss et al., 1992a; Hayes, 1994; Shields and Veizer, 2002; Eq. (1)) suggest that the proportion of total carbon buried as organic matter has been more or less consistent throughout Earth history, both before and after the rise of atmospheric O_2 [2.45–2.32 billion years before present (Ga); Farquhar et al., 2000; Wing et al., 2002; Bekker et al., 2004]. If this is even broadly correct, the carbon cycle must have delivered oxidized equivalents to the oceans and atmosphere throughout much of its history (e.g. Kump et al., 2001; Holland, 2002; Hayes and Waldbauer, 2006).

Estimates of organic carbon burial (and thus oxidant production), however, are only as accurate as the models used to generate them. Bjerrum and Canfield (2004) reexamined the burial history of organic matter with a more detailed isotopic mass balance model that included a third carbon sink, precipitation of carbonate salts within seafloor basalts during submarine weathering (Eq. (3)):

$$f_{org} = \frac{\delta^{13}C_{carb} - \delta^{13}C_{input} + \lambda\Delta_s}{(\delta^{13}C_{carb} - \delta^{13}C_{org}) + \lambda\Delta_s} \quad (3)$$

In their formulation, λ depicts the fraction of inorganic carbon removed by basalt carbonatization, and Δ_s represents the difference in isotopic composition between carbonates associated with ocean floor basalts and carbonates precipitated in shallow water. As λ becomes negligible, or if the isotopic composition of basalt carbonates approaches $\delta^{13}C_{carb}$, Eq. (3) approximates the standard model (Eq. (1)). Although difficult to measure from the geologic record, the two degrees of freedom added by Bjerrum and Canfield (2004) were justified indirectly on the basis of geological observations. Deposition of carbonate minerals within the upper oceanic crust is currently recognized as an important carbon sink (Staudigel et al., 1989; Alt and Teagle, 1999), and was likely significant during Archean time (Walker, 1990; Sleep and Zahnle, 2001). This sink takes on special importance because a number of previous studies had recognized a large difference in carbon isotope ratios between shallow water stromatolitic dolomites ($\delta^{13}C_{carb} \sim 0$‰ VPDB) and coeval siderites within deep-water iron formation ($\delta^{13}C_{carb} \sim -5$ to -7‰) in Late Archean to Paleoproterozoic successions (Becker and Clayton, 1972; Perry and Tan, 1972; Beukes et al., 1990; Kaufman et al., 1990; Winter and Knauth, 1992; Ohmoto et al., 2004); the observed difference was attributed to a strong isotopic gradient within the water column. These observations fueled Bjerrum and Canfield's hypothesis that during Archean time, carbonate formed during submarine basalt alteration would have been depleted in ^{13}C, providing an important but previously unrecognized sink for isotopically light carbon that causes the standard model (Eq. (1)) to overestimate the proportion of carbon buried as organic matter. Bjerrum and Canfield's (2004) revised estimates of f_{org} vary between 0 and 0.10. A corollary of these results is that the proportion of oxidizing equivalents released by Archean organic matter burial could have been far less than previously thought. If correct, the analysis by Bjerrum and Canfield (2004) offers a potential solution to the "Late Archean oxygen problem" by alleviating tension between lipid biomarker data that place cyanobacterial oxygenic photosynthesis within the Archean Eon (Brocks et al., 2003a,b; Waldbauer et al., this volume) and other geological and geochemical proxies that suggest an O_2 mixing ratio $\ll 10^{-5}$ in the contemporaneous atmosphere and oceans (Rye and Holland, 1998; Rasmussen and Buick, 1999; Farquhar et al., 2000; Pavlov and Kasting, 2002).

Did a strong carbon isotopic gradient exist in ocean basins prior to the appearance of environmental oxygen? Previous work from the Pethei carbonate platform (deposited circa 1.9 Ga) of the Great Slave Lake Supergroup revealed that if any carbon isotopic gradient existed between shallow and deep-water stratigraphic sections, it was slight (<0.5‰) (Hotinski et al., 2004). But was this also the case in Late Archean oceans? If so, what then accounts for the observed difference in carbon isotope ratios between basinal siderites and shallow water stromatolites? Here, we report carbon isotopic data from a Late Archean carbonate platform and banded iron formation succession preserved with a depth transect along the western margin of the Kaapvaal Craton in South Africa, providing direct constraints on these issues. In addition, we use a simple mathematical model to explore the conditions under which a 6‰ $\delta^{13}C$ oceanic gradient might emerge and ask whether those criteria could reasonably have been met, given our (admittedly limited) understanding of Late Archean ocean chemistry, biology, and climate.

As well as providing information about the organic carbon burial fraction of the ancient carbon cycle, subtle variations in carbon isotopic ratios of sedimentary organic matter reveal complex interactions between environmental chemistry and biochemistry. Diverse mechanisms for fixing organic matter (Calvin cycle, reverse tricarboxylic acid cycle, 3-hydroxypropionate cycle, and reductive acetyl-CoA pathway) fractionate carbon isotopes to different degrees (Hayes, 2001). Heterotrophs, particularly those with fermentative metabolisms, further affect the isotopic compositions of organic carbon. On top of this, post-depositional diagenetic processes may alter original organic $\delta^{13}C$ values dramatically. The primary challenge is therefore to de-convolve the effects of these processes on ancient sedimentary organic matter.

Late Archean kerogens include some of the most ^{13}C-depleted carbon isotopic values measured in the entire stratigraphic record (Schoell and Wellmer, 1981; Strauss et al., 1992a; Strauss and Moore, 1992; Eigenbrode and Freeman, 2006). It has been suggested that these light $\delta^{13}C$ values developed in ecosystems where a significant proportion of the carbon incorporated into biomass derived from biogenic methane (Hayes, 1994; Hinrichs, 2002). Anomalously low $\delta^{13}C$ values have been documented previously from the Transvaal Supergroup on the Kaapvaal Craton (Beukes et al., 1990; Strauss and Beukes, 1996). Do these values constrain biosynthetic mechanisms in the Late Archean? How strong is the evidence for secondary recycling? And how were depositional values later affected by diagenesis? We report new organic carbon isotopic data arranged within a sequence stratigraphic framework that samples a variety of paleoenvironments and different host lithological units. These data allow us to explore the geological context of isotopically light Archean organic matter.

2. Oceanic carbon cycle mathematical model

All biogeochemically significant elements and isotopes in the oceans are distributed as a function of both ocean circulation (mixing) and the biological pump, referred to here as the production and vertical export of biogenic particles from surface waters to the deep oceans. Dynamics within modern ocean basins maintain a water-column carbon isotopic gradient of approximately 2‰ (Kroopnik, 1980; Broecker and Peng, 1982), sustained in part by the fixation of carbon in the surface ocean, the sinking of biomass from the mixed layer, and the subsequent remineralization of organic matter at depth. Collectively, these processes result in a net transfer of isotopically light carbon to the deep oceans. The biological pump acts to increase the water column isotopic gradient, while circulation of dissolved inorganic carbon (DIC) serves to dampen it. In this section we encode these intuitive relationships within a theoretical isotopic mass balance model of the oceanic carbon cycle, building on previous work from Broecker and Peng (1982) and Kump (1991). This mathematical formulation is useful because it compels biogeochemical arguments to remain internally consistent while allowing the efficient exploration of parameter space, as well as the generation of testable quantitative predictions. What set (or sets) of boundary conditions would produce a large (5–7‰) $\delta^{13}C$ gradient, and are these conditions consistent with estimates from first principles about the carbonate chemistry and biology of Late Archean oceans?

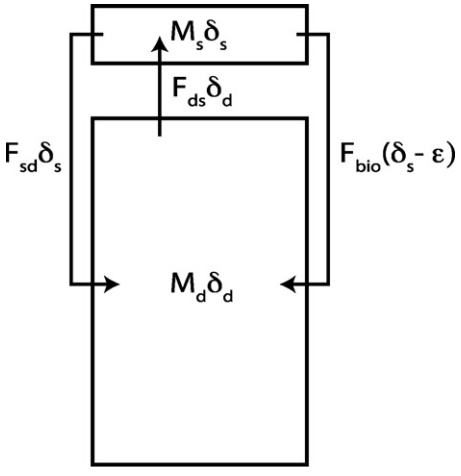

Fig. 1. The internal dynamics of the oceanic carbon cycle captured by the topology of a theoretical isotopic mass balance mathematical model.

Fig. 1 shows the model's topology. Two reservoirs are resolved, representing the mass of carbon in surface (M_s) and deep oceans (M_d), respectively. Three fluxes exchange carbon between these pools. The surface communicates with the deep reservoir via the biological pump (F_{bio}) and advection of inorganic carbon during mixing (F_{sd}). Carbon from the deep pool is returned to the surface oceans, also during mixing (F_{ds}). Each reservoir carries information about its isotopic composition; δ_s and δ_d describe the $\delta^{13}C$ of the surface and deep reservoirs, respectively. The isotopic composition of the biological pump flux is determined by the $\delta^{13}C$ of the surface ocean (δ_s), offset by a factor ε, which derives from the kinetic isotope fractionation incurred during carbon fixation. Our model is required to maintain both mass balance:

$$\frac{dM_s}{dt} = F_{ds} - F_{sd} - F_{bio} \tag{4}$$

$$\frac{dM_d}{dt} = F_{sd} + F_{bio} - F_{ds} \tag{5}$$

and isotopic mass balance:

$$\frac{dM_s\delta_s}{dt} = F_{ds}\delta_d - F_{sd}\delta_s - F_{bio}(\delta_s - \varepsilon) \tag{6}$$

$$\frac{dM_d\delta_d}{dt} = F_{sd}\delta_s + F_{bio}(\delta_s - \varepsilon) - F_{ds}\delta_d \tag{7}$$

In order to explore the behavior of a long-lived oceanic phenomenon (on the order of tens to hundreds of millions of years, far greater than estimates of the residence time of carbon in Archean oceans), our model is allowed to operate at steady state. Solving Eqs. (4)–(7) at steady state yields the following:

$$F_{ds} = F_{sd} + F_{bio} \tag{8}$$

$$F_{ds}\delta_d = F_{sd}\delta_s + F_{bio}(\delta_s - \varepsilon) \tag{9}$$

Together, Eqs. (8) and (9) describe the difference in carbon isotope ratios between the deep and surface oceans:

$$\delta_d - \delta_s = \left(\frac{F_{bio}}{F_{bio} + F_{sd}}\right)\varepsilon \tag{10}$$

Intuitively, this $\delta^{13}C$ difference is controlled by the fraction of the total carbon flux from surface to deep that originates from the biological pump, amplified by the degree of fractionation during autotrophic fixation (Kump, 1991). Given a typical (though not universal) form 1 ribulose-1,5-bisphosphate carboxylase/oxygenase (RuBisCO) fractionation factor (ε = 25‰; Scott et al., 2004), expression (10) can be solved for a wide array of potential flux parameter values.

Fig. 2 illustrates the results of model calculations for the isotopic difference between the deep and surface carbon reservoirs contoured against fluxes of DIC downwelling (F_{sd}) and the biological pump (F_{bio}), both in mol C year^{-1}. Although estimates of modern DIC and particulate organic carbon fluxes vary (e.g. Broecker and Peng, 1982; Sundquist, 1985; Jahnke, 1996), they are consistent with model calculations of a 2‰ inter-reservoir isotopic difference in present day oceans ($F_{sd} = 3.0 \times 10^{15}$ mol C year^{-1}, $F_{bio} = 2.5 \times 10^{14}$ mol C year^{-1}). As a benchmark, this demonstrates that our model broadly captures the vertical behavior of the oceanic carbon cycle. In order to obtain a 6‰ gradient within modern ocean basins, the oceans would have to contain far less DIC or, alternatively, the biological pump would have to increase nearly 4-fold.

Few primary data exist on the strength of the biological pump in earlier oceans; but there are good reasons to suggest that it was, if anything, weaker than today. The physical characteristics of particulate organic matter determine rates of sinking from the surface ocean. Small particles, ranging in size from 1 to 12 μm, sink extremely slowly if at all (rates on the order of 0–0.1 m d^{-1}; McCave,

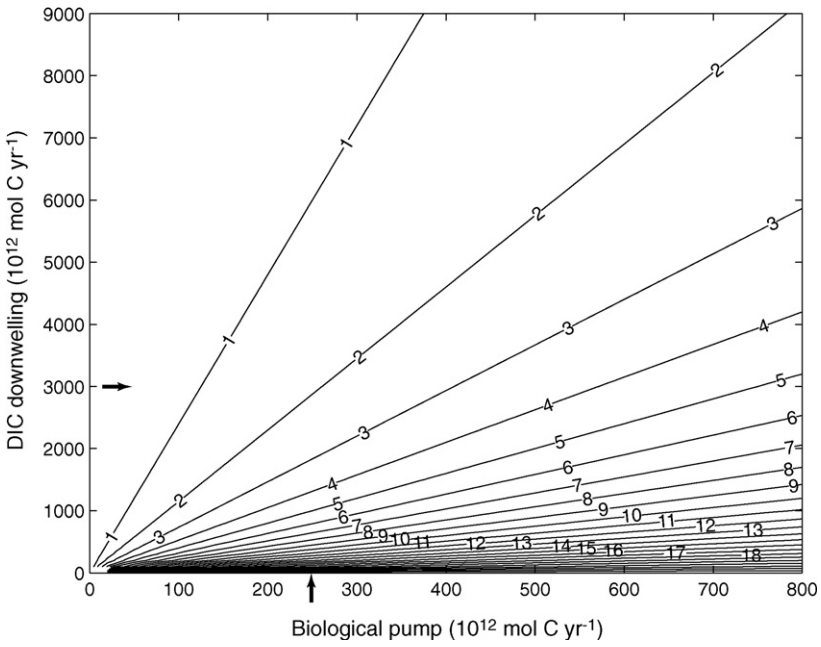

Fig. 2. Contour plot (contour units in ‰) of the absolute differences between the $\delta^{13}C$ of the surface and deep ocean carbon reservoirs plotted as a function of DIC downwelling (F_{sd}) and biological pump (F_{bio}) fluxes. Calculated from Eq. (10). Arrows point to estimates of modern flux values.

1975). The biological pump therefore is made up of large sinking particles, fecal pellets, and amorphous aggregates. Zooplankton fecal pellets contribute to this flux, but the chief proportion is composed of marine snow and phytoplankton aggregates (Turner, 2002). The small density contrast between the organic components of the particulate flux (1.025 g cm^{-3} (Smayda, 1970)) and surrounding seawater (1.024 g cm^{-3}) demands the presence of mineral ballast to assist in sinking. During the Precambrian (and, indeed, before the mid-Mesozoic) few phytoplankton produced mineralized skeletons that could provide ballast to drive the biological pump, leaving only lithogenic particles to aid in sinking. More specific to the Late Archean, it has been argued that before either the evolution or widespread use of oxygenic photosynthesis, total primary production would have been significantly lower because of strong phosphorus limitation or limited supply of electron donors (Bjerrum and Canfield, 2002; Canfield, 2005; Kharecha et al., 2005; Canfield et al., 2006). Consequently, it is unlikely that the biological pump in late Archean oceans was stronger than today's; the reasoning presented above suggests that it was probably less effective.

Is it possible then that Archean oceans contained less DIC than they do today? According to stellar evolution models, the Sun's luminosity has increased on the order of 25% over the age of the solar system; to reconcile this inference with geological observations of ancient liquid water, it was suggested that greenhouse gases (Sagan and Mullen, 1972), in particular CO_2 (Owen et al., 1979; Walker et al., 1981) in Archean air were present in much greater concentrations than today. Accepting that the partial pressure of CO_2 was higher at 2.7–2.5 Ga than it is today, how would this have been reflected in ocean DIC concentrations?

The carbonate system consists of six variables ([CO_2], [HCO_3^-], [CO_3^{2-}], [H^+], DIC, and total alkalinity), and specific knowledge of any two is required to solve for the others. The ancient carbonate system has commonly been explored through the application of a simple calcite equilibrium model (Holland, 1972; Walker, 1983; Grotzinger and Kasting, 1993; Hotinski et al., 2004), an approach that requires several assumptions: (1) the oceans were at equilibrium (or several times supersaturated) with respect to calcite, (2) knowledge of [Ca^{2+}] (often fixed at modern ocean concentrations), and (3) the activities of chemical species equaled their concentrations in seawater. The advantage to this procedure is that it is well supported by the ubiquity of marine carbonates in the geologic record. Its disadvantage is that the calcium concentrations of ancient oceans are little understood, and the solubility product constants underpinning such models can vary considerably, stemming in part from differences in the activity coefficients between Ca^{2+} and CO_3^{2-} (Stumm and Morgan, 1996; Zeebe and Wolf-Gladrow, 2001). For this reason, a different approach is taken here. By fixing [H^+], our model can be solved for a variety of P_{CO2} values. The calculation uses Henry's law, first, and second acidity constants, at T = 25 °C, P = 1 atm, and S = 35 (Zeebe and Wolf-Gladrow, 2001). Although the exact average pH of the Late Archean oceans remains unknown, this exercise can be iterated for a range of plausible values. Fig. 3 illustrates calculations of the difference in carbon isotope ratios between the deep and surface ocean reservoirs as a function of the biological pump (F_{bio}) and P_{CO_2}, at four different pH values. Again, the model correctly describes a 2‰ inter-reservoir isotopic difference at pH 8.08, consistent with estimates of internal carbon fluxes in modern oceans. At higher pH (favoring HCO_3^- and CO_3^{2-}) the oceans contain more DIC, resulting in a larger F_{sd} flux and, thus, smaller isotopic differences. At lower pH the opposite occurs. Simulations from one dimensional atmospheric climate models suggest that the low-end estimate of P_{CO_2} for the Late Archean atmosphere would be approximately 10^4 μatm (Kasting, 1987, 1993). At or above this P_{CO_2}, our model predicts large carbon isotopic gradients only at strikingly low ocean pH values. If such low pH oceans ever existed, they would have required extraordinarily high Ca^{2+} concentrations to account for the widespread production of calcium carbonate in Archean sedimentary basins (Grotzinger and Kasting, 1993).

The calculations and reasoning presented here suggest that under conditions characterized by high P_{CO_2} and moderate ocean pH, a strong vertical carbon isotopic gradient in Late Archean ocean basins is unexpected, particularly if the biological pump was no stronger than modern. While it is possible that there were additional processes ignored here (it has, for example, been speculated that ^{13}C-depleted hydrothermal plumes influenced deep water carbon chemistry; Beukes et al., 1990) that contributed to isotopic differences within the water column, a 6‰ $\delta^{13}C$ gradient, sustained globally, seems unlikely. What, then, explains the consistent finding

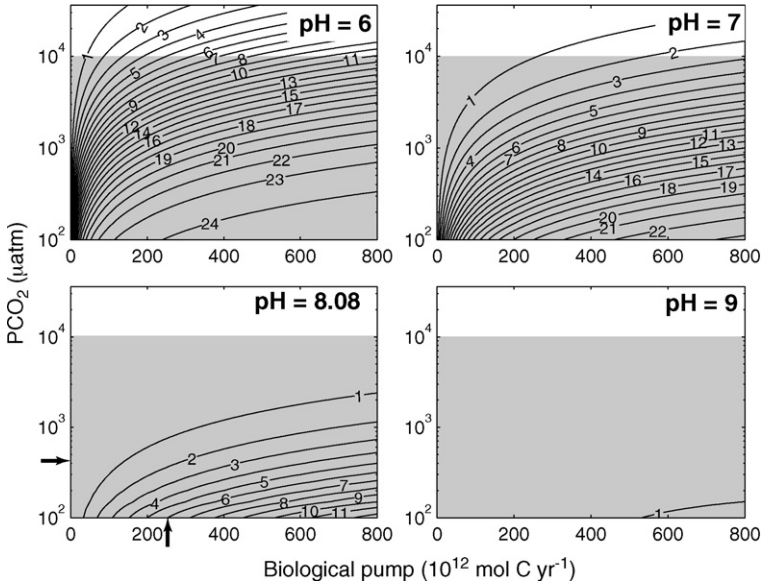

Fig. 3. Contour plots of the absolute differences between the $\delta^{13}C$ of the surface and deep ocean carbon reservoirs plotted as a function of P_{CO_2} (translated into an F_{sd} flux) and biological pump fluxes calculated for pH 6, 7, 8.08, and 9. Arrows point to estimates of modern flux values for pH 8.08. Unshaded portion denotes parameter space compatible with climate model P_{CO_2} estimates.

of strong isotopic difference between shallow marine carbonates and siderites in basinal iron formations? In the following section this question is explored directly, using carbon isotope data from several deep drill cores sampled along a depth transect perpendicular to the margin of a Late Archean carbonate platform.

3. Campbellrand–Kuruman sedimentary succession

In South Africa, the Late Archean to Paleoproterozoic Transvaal Supergroup is preserved in two distinct structural basins (Griqualand West and Transvaal proper) over an area of 200,000 km^2; the original deposit likely extended across the entire 600,000 km^2 surface of the Kaapvaal Craton (Fig. 4; Button, 1973; Beukes, 1987; Sumner, 1995). The Transvaal succession sits disconformably atop volcanic and intercalated sedimentary rocks of the Ventersdorp Supergroup (felsic volcanics from the upper Ventersdorp yielded a U-Pb ion microprobe age from zircon of 2714 ± 8 Ma; Armstrong et al., 1991). Thermal subsidence after the heating and thinning of the Kaapvaal Craton during Ventersdorp accumulation likely afforded the accommodation space necessary for deposition of the Transvaal Supergroup (Schmitz and Bowring, 2003; Sumner and Beukes, 2006).

In Griqualand West, three distinct subgroups of the Transvaal Supergroup have been recognized. The Schmidtsdrif Subgroup consists of mixed siliciclastic and carbonate units with an inferred maximum age between 2642 ± 3 Ma and 2664 ± 1 Ma, based on correlation with units elsewhere in the basin (Barton et al., 1995; Walraven and Martini, 1995). Resting conformably on top of the Schmidtsdrif, the ~2588–2520 Ma (Barton et al., 1994; Sumner and Bowring, 1996; Altermann and Nelson, 1998) Campbellrand Subgroup is represented by an areally extensive, ~2 km thick marine platform. The platform began as a carbonate ramp flanking siliciclastic tidal flats along basement highs and developed into a mature rimmed carbonate shelf that spread across the entire Kaapvaal Craton (Beukes, 1987). Eventually the carbonate platform drowned during a major transgression, reflected in the deposition of the ~2460 Ma (Pickard, 2003) Kuruman Iron Formation (Beukes, 1984). In general, the Campbellrand platform and Kuruman Iron Formation appear to reflect the passive accumulation of chemical precipitates on thinned continental crust (marine platform) adjacent to a major Late Archean ocean basin.

Today the Campbellrand–Kuruman sedimentary succession is essentially undeformed across much of the ancient craton. Steeper dips occur around the Bushveld Igneous Complex, and acute folding and faulting appears along the western edge of the craton, where Proterozoic red beds of the Olifantshoek Group are thrust over Campbellrand rocks (Stowe, 1986; Beukes, 1987; Beukes and Smit, 1987). Significant metamorphism is limited locally to rocks near the Bushveld complex; the rest of the Campbellrand is below greenschist facies equivalent (Button, 1973; Miyano and Beukes, 1984). Textures within the rocks are commonly well preserved by fabric-retentive, early diagenetic dolomite (Sumner and Grotzinger, 2000).

Within the Campbellrand–Kuruman sedimentary succession, it is possible, in principle, for any given time horizon to trace paleoenvironments laterally from shallow water tidal flats, populated with stromatolites, oolitic grainstones, and pseudomorphs of aragonite crystal fans, into slope and basinal microbialites, turbidites, mudstones, and iron formation deposited in deep water (several hundred m to >1 km water depth). The Campbellrand–Kuruman stratigraphy is locally well exposed, but key areas, including the platform to basin transition, are not. An intact slice of the Campbellrand platform margin can be found in Griqualand West, 25–100 km northeast of Prieska. Campbellrand–Kuruman rocks are well preserved in this area (particularly for Archean sediment), though their flat-lying orientation is both a blessing and a curse. In order to examine the platform to basin transition, the Agouron Drilling project (http://agouron.spectraconsulting.co.za) collected two deep diamond drill cores from this area, one from the paleogeographic upper slope (GKF01), and the second from the paleogeographic lower slope (GKP01) (Fig. 4). Samples from these fresh drill cores were supplemented with material from an existing proprietary drill core capturing shallow water platform paleoenvironments (BH1-Sacha). Data from these three cores permit the investigation of compositional differences between carbonates deposited across a wide range of water depths, in a sedimentary basin that also accumulated iron formation beneath its deepest waters.

A generalized stratigraphy of the Transvaal Supergroup in the Griqualand West basin, including projected locations of the three drill cores, is shown in a northeast to southwest trending cross section in Fig. 5. Detailed descriptions of the sequence stratig-

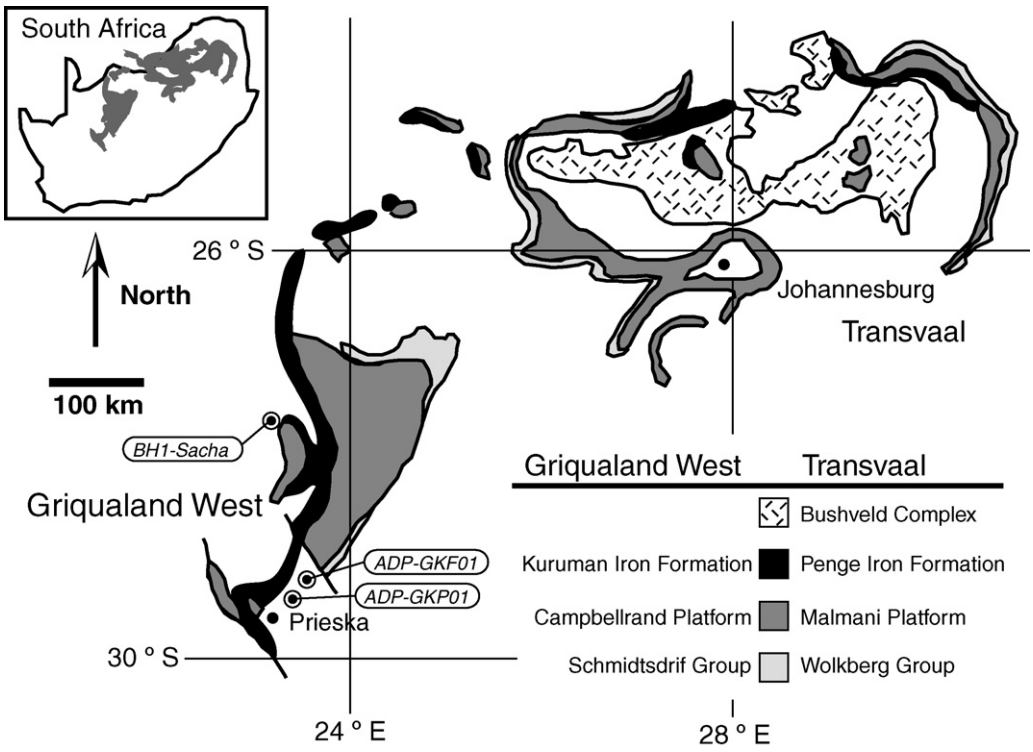

Fig. 4. Geological map of the Transvaal Supergroup preserved on the Kaapvaal Craton, modified from Sumner and Beukes (2006). A segment of the Campbellrand Platform margin is preserved in the Griqualand West structural basin. Locations of the drill cores GKP01, GKF01, and BH1-Sacha are labeled.

raphy, lithological units, sedimentology, and major, minor, and trace element geochemistry of the two Agouron cores (GKP01 and GKF01) can be found in Schröder et al. (2006) and Sumner and Beukes (2006). The sedimentology of BH1-Sacha is described by Altermann and Siegfried (1997). To facilitate discussion, however, salient points of the sedimentary geology are summarized here. The Vryburg Formation records the first post-Ventersdorp marine trangression of the Kaapvaal Craton in Griqualand West. The lower part consists primarily of ripple-laminated sandstones that deepen upwards into pyritic shales and turbidites. The contact between the Vryburg and Boomplaas formations is gradational, characterized by shale and thin carbonate interbeds with increasing carbonate content up section. Declining siliciclastic flux during high stand was followed by progradation of a short-lived carbonate platform, the Boomplaas Formation, into the basin. Throughout the extent of the study area, Boomplaas carbonates are always shallow-water deposits characterized by columnar, digitate, and domal stromatolites, cross-bedded oolitic grainstones (with local cm-scale ooids), and edgewise conglomerates. Another transgressive sequence began on top of the Boomplaas platform, represented by deposition of the Lokammona Formation, organic-rich pyritic shales occasionally interbedded with carbonate grainstones interpreted as mass flow deposits. Again, carbonate content increases toward the gradational upper contact with the overlying Monteville Formation, a steepened carbonate ramp that developed during presumed high stand. Following Monteville deposition, the entire Kaapvaal Craton was flooded, establishing widespread carbonate deposition and development of the steep-margined Campbell-

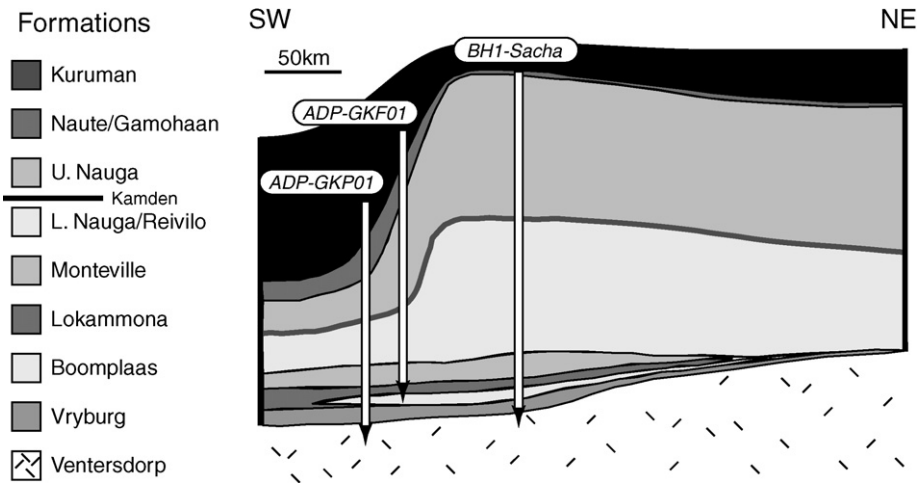

Fig. 5. A northeast–southwest trending cross-section reveals the generalized stratigraphy of the Transvaal Supergroup across the Campbellrand Platform margin. Formations are listed in stratigraphic order. The approximate locations and stratigraphy captured by the three drill cores are illustrated.

rand Platform. The platform can be broadly divided into two large sequences, the Lower Nauga/Reivilo and the Upper Nauga formations, each representing aggradational packages separated by a striking thin transgressive unit comprised in part by the Kamden Member at the top of the Lower Nauga/Reivilo Formation. Near the top of the Lower Nauga/Reivilo Formation, there was pronounced deepening across the platform, which began with the deposition of deep subtidal, fenestral microbialites and culminated in the accumulation of siderite and hematite facies iron formation (the Kamden Member). Carbonate deposition was then reestablished by the Upper Nauga Formation, which inherited the original margin location. During Upper Nauga time, the Campbellrand Platform slope was at its steepest, with a lagoon that developed episodically behind the reef margin. Beginning with the Naute/Gamohaan formations, a major transgression led to the ultimate demise of the Campbellrand Platform, as carbonate deposition was slowly outpaced by accommodation. The Naute/Gamohaan formations are characterized by deep subtidal fenestral microbialites and shales with increasing chert content that ultimately grade into iron formation of the Kuruman Formation, which accumulated across the entire Kaapvaal Craton. At their tops, all three cores contain an erosional unconformity where Permian tillites of the Karoo Supergroup incised into the Transvaal sequence. In GKP01 and GKF01 the lower Kuruman Formation is still preserved, however in BH1-Sacha, the Kuruman Formation was removed altogether and the young tillites rest directly on Gamohaan Formation microbialites.

Differences in paleoenvironmental water depth among BH1-Sacha, GKF01, and GKP01 vary significantly throughout the stratigraphy. During deposition of the Boomplaas Formation, all three cores capture approximately the same shallow water facies. This changed dramatically, however, as the Campbellrand Platform developed. The strongest contrast between water depths at the three core locations occurred during the deposition of the Lower and Upper Nauga formations, and likely continued through the transition to iron formation. Differing accumulation rates led to stratigraphic thicknesses that are greatest on the platform and thin considerably across the margin toward the basin (dip-corrected thickness ratios between BH1-Sacha, GKF01, and GKP01 are approximately 10:4:3). Estimates of absolute water depths are uncertain. The intertidal to shallow subtidal facies contained in BH1-Sacha suggest deposition from very near sea level to several meters water depth. The Campbellrand–Kuruman stratigraphy present in the two Agouron cores above the Monteville Formation lacks evidence of wave-influenced sedimentary structures; the only sedimentary grains present in these sections are associated with gravity flow deposits, indicating that both cores capture sub-wave base environments. Assuming that the Campbellrand Platform attained a typical marine slope profile (Adams and Schlager, 2000), it is possible to estimate water depths from the location of the cores with respect to the orientation of the platform margin. Conservatively, a slope of 4° results in potential water depths of several hundred meters in GKF01 to greater than 1 km for the distally positioned GKP01. Other estimates derived from comparisons of stratigraphic thicknesses suggest water depths somewhat shallower (Klein et al., 1987). Nonetheless, in modern ocean basins the largest of rate of change in the $\delta^{13}C$ of seawater occurs through the mixed layer (in the upper <250 m of the water column, and often shallower; Broecker and Peng, 1982). If a strong carbon isotopic gradient existed, it should be captured among BH1-Sacha, GKF01, and GKP01. In addition to the differences in water depth among the three core locations, each individual core records an overall deepening-upward trend into iron formation depositional environments as the carbonate platform was progressively drowned. This provides an additional means of capturing different paleoenvironmental water depths.

Ancient sedimentary successions can only record an isotopic depth gradient if carbonates deposited at depth were precipitated in place and not transported from shallow sources (e.g. Hotinski et al., 2004). In younger depositional systems, this condition is generally not met; carbonate was produced in shallow water environments and subsequently advected to sites undergoing active sedimentation. In the Campbellrand–Kuruman sedimentary succession, however, seafloor carbonate precipitates occur throughout the depth profile, where they commonly constitute a major fraction of the total carbonate (Sumner, 1995, 1997a,b; Sumner and Grotzinger, 1996a,b, 2004; Schröder et al., 2006; Sumner and Beukes, 2006). This *in situ* precipitation, coupled with a stratigraphic framework that samples a large range of paleoenvironmental water depths in both space and time, provides the sampled needed to examine $\delta^{13}C$ distributions as they once existed in the water column of a Late Archean ocean basin.

4. Carbon isotope analysis

4.1. Carbonate carbon

GKP01 and GKF01 samples were obtained for isotope analysis from splits of whole rock samples for which elemental data were also measured (Schröder et al., 2006). Samples were collected from the cores at approximately 5 m intervals and ground into powder in an agate vibratory disc mill, with a slice retained for thin section analysis. In addition to the whole rock analyses, a number of samples were collected at tighter intervals by microdrilling several mg of powder from specific laminations, avoiding any secondary veining. During the microsampling of iron formation carbonates care was taken to target fine-grained siderite-rich laminations, avoiding (late diagenetic) coarse-grained rhombohedral ankerite and ferroan-dolomite. Carbonate $\delta^{13}C$ and $\delta^{18}O$ values were measured concurrently on a VG Optima dual inlet mass spectrometer fed by an isocarb preparation device in the Harvard University Laboratory for Geochemical Oceanography. Many of the samples measured from the cores were composed of dolomite. To avoid memory effects associated with dolomite analyses, longer reaction and sample pump out times were used. Carbonate samples (~1 mg) were dissolved in a common anhydrous H_3PO_4 bath kept at 90 °C for 8 min. Evolved CO_2 was purified and captured cryogenically, then measured against an in-house reference gas. Typical analytical uncertainty was ±0.1‰. Results were calibrated and reported with reference to Vienna Pee Dee Belemnite using a laboratory Cararra Marble standard. Six measurements of the laboratory standard were made within every run of 54 samples.

Carbonates from BH1-Sacha were analyzed in the Environmental Isotope Group at iThemba Labs, South Africa. Samples were reacted following a technique modified after McCrea (1950) with 10–11 mg of each sample and 2 ml of 100% H_3PO_4. After equilibration, samples were reacted at 25 °C for calcite and 50 °C for dolomite overnight. The evolved CO_2 gas was finally collected in reusable sample bottles or break-seal tubes. Liberated CO_2 was pumped through cold traps using dry ice and liquid nitrogen in order to remove water and other condensable gases. Isotope analyses were performed on a Finnigan MAT-251 gas-source mass-spectrometer against a working gas from a commercial CO_2 cylinder. Internal laboratory standards were included in each batch of samples, calibrated against NBS19 as international reference. Isotopic compositions are given in standard delta notation relative to VPDB. The calibration of the working gas was done by analyzing international reference materials using NBS19, which is defined as reference Vienna-PDB by: $\delta^{13}C_{NBS19}$/VPDB = 1.95‰ (Hut, 1987). Repeated analysis of internal standards (MHS1, MDS1 and MD4) yielded values in an interval of ±0.1‰ (1σ) for $\delta^{13}C$ values. Reproducibility on replicate analyses is expected to be better than 0.1‰

(aliquot difference of a duplicate analysis). This could be achieved in all cases, save for a few exceptions. In these cases, an aliquot spread of <0.2‰ had to be accepted. These values, however, still lie within a ±0.1‰ (1σ) space around the average of a duplicate analysis.

4.2. Organic carbon

Abundances of total carbon (TC) and total inorganic carbon (TIC) were measured on whole rock powder samples from GKP01 and GKF01 with a CS-MAT 5500 for solids using NDIR spectroscopy. Total organic carbon (TOC) abundances were calculated as difference between TC and TIC. Analytical errors were ≤2%. For organic carbon isotope measurements, CO_2 was prepared via sealed tube combustion of carbonate-free rock powder (Strauss et al., 1992b). Isotope measurements ($\delta^{13}C_{org}$) were performed with a Finnigan Delta-plus mass spectrometer, equipped with a dual-inlet system. International reference material USGS 24 and several laboratory standards (paper shale, brown coal, and anthracite) were used for calibration. Carbon isotope results are reported in the standard delta notation as per mil difference from the Vienna Peedee Belemnite standard. Reproducibility, as determined through replicate measurements, was better than ±0.2‰.

5. Results

5.1. Carbonate carbon

Fig. 6 illustrates the detailed stratigraphy of GKP01, GKF01, and BH1-Sacha plotted against carbonate $\delta^{13}C$ values. The vertical scale for BH1-Sacha is one half that of GKP01 and GKF01, which appear at the same scale. In order to compare isotope ratios between the three cores, two lines of correlation are drawn. The datum used to align the cores was the flooding of the Boomplaas carbonate platform. An additional line of correlation was drawn through the iron formation of the Kamden Member of the Lower Nauga/Reivilo Formation, a robust lithologic and sequence stratigraphic marker present in all three cores. Because of both the steep platform margin geometry attained during post-Kamden time and the presumed time-trangressive nature of the deepening into the Kuruman Formation, it is difficult to correlate in an absolute sense between the platform top and slope/basinal stratigraphic sections above this horizon (Sumner and Beukes, 2006). Nonetheless, we have confidence that water depths increase both along timelines from northeast to southwest, and upsection among and within BH1-Sacha, GKF01, and GKP01.

Carbonate $\delta^{13}C$ data from the three drill cores tend to cluster around a mean value of −0.5‰ throughout the Campbellrand Platform (both between cores and within cores), indicating that the isotopic composition of water column DIC within this ocean basin was nearly uniform with depth. Noticeable deviations toward lighter isotopic values do, however, occur in specific horizons. These are prevalent in the mixed siliciclastic carbonate sections near the bottom of all three cores, and at the top of GKP01 and GKF01, but are rare within thick platform carbonate. These horizons are characterized lithologically by a prevalence of shale, tend to be relatively carbonate poor (e.g. ^{13}C-depletion at ~480 m in GKP01), correlate with high weight percent iron (Schröder et al., 2006), and commonly demonstrate cm-scale $\delta^{13}C$ variability of >1.0‰. Iron formation lithologies contain the strongest ^{13}C-depletion. Carbon isotope ratios of carbonate in siderite-rich iron formation are highly variable, with $\delta^{13}C$ values that range from −0.5‰ to as low as −15‰. This is documented clearly in GKF01 in the vicinity of the Kamden Member. Microbialite facies above and below the Kamden iron formation have $\delta^{13}C$ values tightly grouped around −0.5‰. Within the iron formation *sensu strictu*, the isotopic composition of siderites

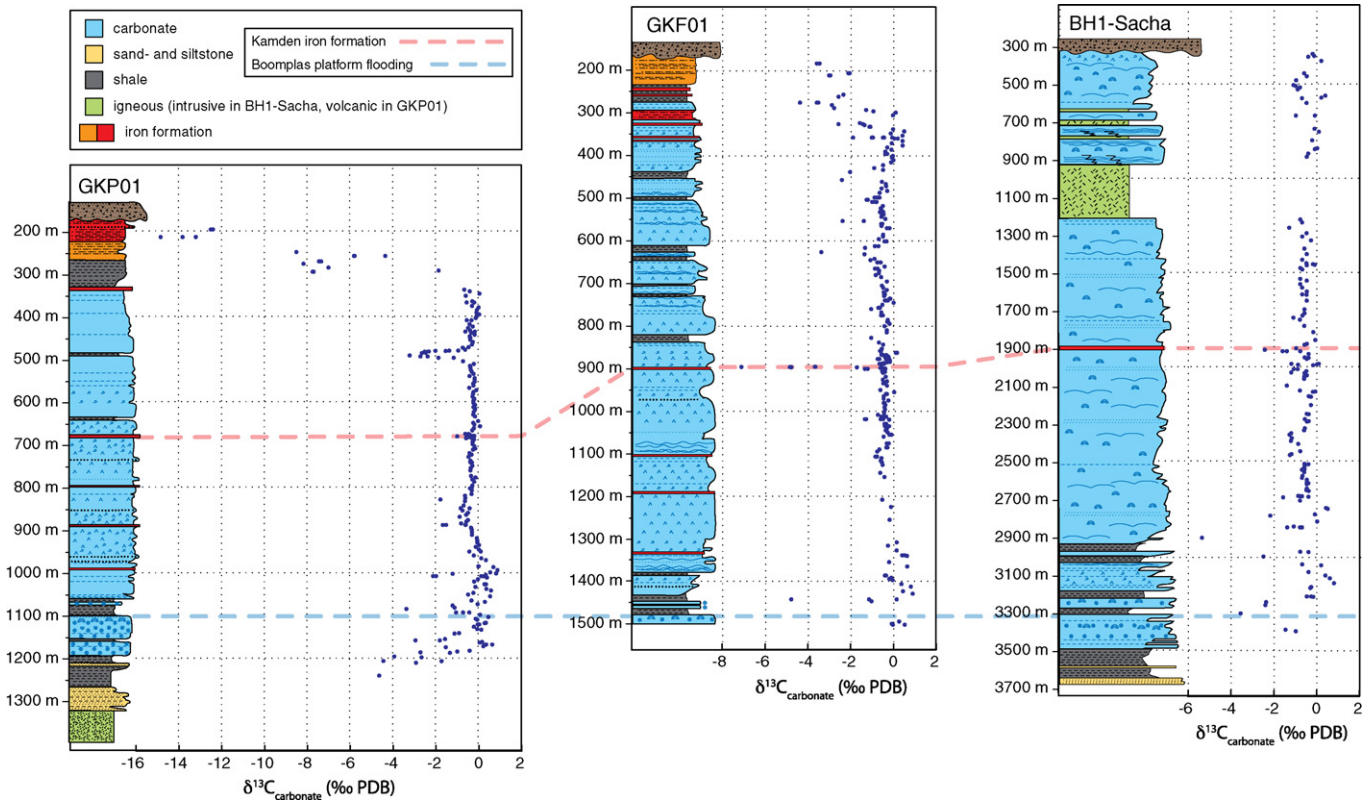

Fig. 6. Carbonate $\delta^{13}C$ data plotted against the detailed stratigraphy from drill cores GKP01, GKF01, and BH1-Sacha. Note the change in scale for BH1-Sacha. Two lines of correlation are drawn, the sequence boundary marked by the flooding of the Boomplaas platform and deposition of the Kamden iron formation.

varies unsystematically on a cm length scale from near water column values of −0.5‰ down to −7.6‰.

5.2. Carbonate oxygen

Oxygen isotope ratios of carbonate minerals can provide a measure of post-depositional alteration. $\delta^{18}O$ data for GKP01 and GKF01 appear in Fig. 7A. GKP01 $\delta^{18}O$ values range from a low of −16.7‰ to a high of −5.5‰, with a median value of −8.5‰. GKF01 $\delta^{18}O$ displays a spread from −10.8 to −5.5‰, median value of −7.6‰. These values are similar to those measured previously from shallow water Campbellrand stromatolites and the Kuruman iron formation (Beukes et al., 1990), and Archean and Paleoproterozoic carbonates in general (Shields and Veizer, 2002). The $\delta^{18}O$ core depth distributions suggest that GKP01 has experienced greater diagenetic alteration than GKF01, particularly in the shale-rich horizons present below 1000 m and above 500 m. Plots of carbonate $\delta^{18}O$ and $\delta^{13}C$ data for GKP01 and GKF01 are illustrated in Fig. 7B. Carbonates from GKP01 shales show the positive relationship between $\delta^{18}O$ and $\delta^{13}C$ (Fig. 7B, dashed envelope) expected for diagenesis; this is distinct from the low $\delta^{13}C$ values in the iron formation (Fig. 7B, solid envelope), which do not show such a trend. In both cores, the least altered horizons appear to be those associated with the deposition of the thick carbonate sequences of the Lower Nauga/Reivilo and Upper Nauga formations (the same areas for which the $\delta^{13}C$ water depth test is the most explicit).

5.3. Organic carbon

Carbon isotope ratios of organic carbon and total organic carbon (TOC) weight percents of samples from GKP01 and GKF01 are plotted according to the stratigraphy in Fig. 8. Again the two lines of correlation shown are the Boomplaas flooding event and deposition of the Kamden iron formation. Both cores are quite organic rich. TOC ranges from <0.01 to 11.85 wt.%, with mean values of 1.68 and 1.32 wt.% for GKF01 and GKP01, respectively. The highest TOCs occur within the Naute Formation shales; lesser peaks occur at different stratigraphic horizons throughout the Campbellrand Platform.

Carbon isotope ratios of organic matter from these cores show significant variability (on m length scales) and expose several systematic relationships. $\delta^{13}C$ values in GKF01 range from −44.83 to −24.03‰, with a mean of −33.31‰ and a standard deviation of 3.29‰. Similarly, in GKP01, organic carbon $\delta^{13}C$ ranges from −43.94 to −20.38‰, with a mean of −33.66‰ and a standard deviation of 3.85‰. Frequency distributions of $\delta^{13}C$ values from each core appear symmetrical. In GKP01, the stratigraphic trend emerging from the $\delta^{13}C$ data resembles a backwards 'C', with ^{13}C-depleted organics more prevalent in both the shale-rich lower and upper sections of the core. Such a trend does not appear as clearly in GKF01, which does not extend deeply into the siliciclastic-rich lower Schmidtsdrif stratigraphy. In addition to stratigraphic differences, an interesting lithologic pattern exists between the carbon isotope ratios of shales (filled circles) and carbonates (open triangles)

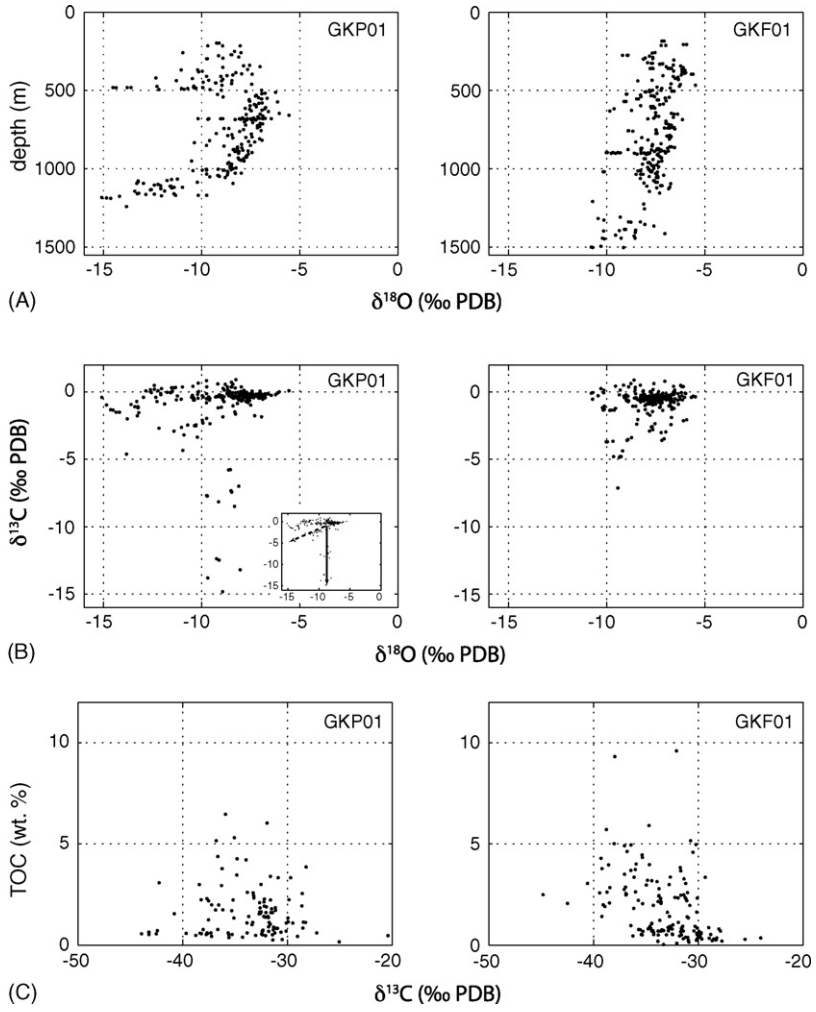

Fig. 7. (A) Carbonate $\delta^{18}O$ variability as a function of depth from GKP01 (left) and GKF01 (right). (B) Crossplots of carbonate $\delta^{18}O$ against $\delta^{13}C$ for GKP01 (left) and GKF01 (right). GKP01 inset, the data are reproduced along with arrays that denote the general behavior of iron formation (solid line) and shale-rich (dashed line) samples, respectively. (C) Crossplots of total organic carbon (TOC) and organic carbon $\delta^{13}C$ for GKP01 (left) and GKF01 (right).

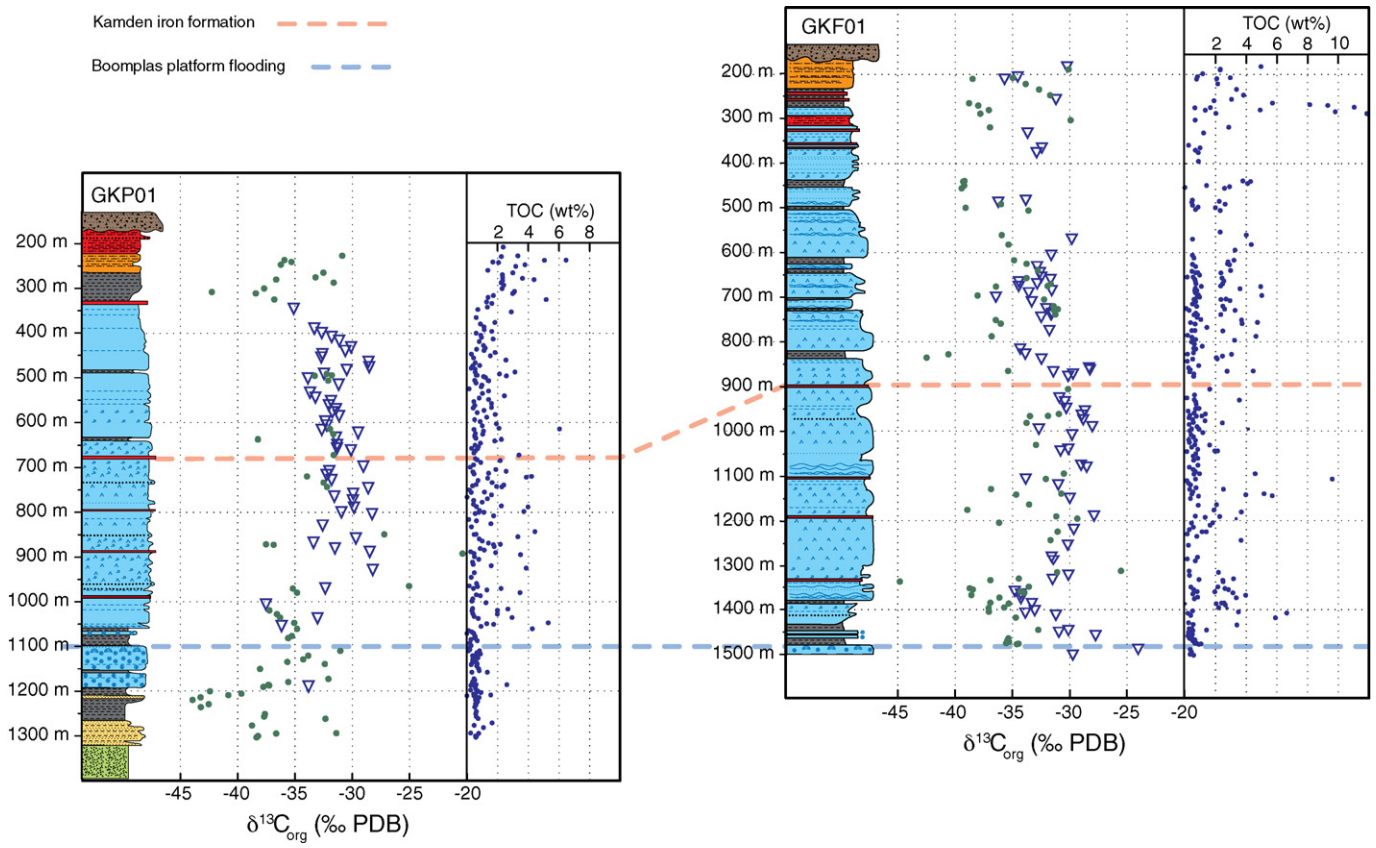

Fig. 8. Organic carbon $\delta^{13}C$ data plotted against the detailed stratigraphy from GKP01 and GKF01. Shales – filled circles, carbonates – open triangles. Again, two lines of correlation are drawn, the sequence boundary marked by the flooding of the Boomplaas platform and deposition of the Kamden iron formation.

in Fig. 8. Shales are commonly >1‰ lighter than stratigraphically adjacent carbonates (particularly in GKF01); rarely do we see the opposite. There does not, however, appear to be a strong relationship between TOC and organic carbon $\delta^{13}C$ (Fig. 7C). GKF01 does reflect a weak correlation at TOC < 1 wt.%, however the relationship breaks down at higher TOCs, and does not really emerge at all in GKP01. $\delta^{13}C$ values from organic matter reveal no significant trend with paleoenvironmental water depth, either between the two cores, or within the deepening upward trend captured within individual cores. Shales deposited in shallow water (e.g. GKP01 1200–1250 m) have a similar organic carbon isotopic composition to those deposited in deep water (e.g. GKP01 ~310 m).

6. Discussion

Much of our current understanding of the Archean Earth system rests on relatively small datasets from one-dimensional studies of specific localities. This previous work provided valuable insights and led to interesting hypotheses (e.g. Hayes, 1994; Bjerrum and Canfield, 2002) proposing that aspects of the Late Archean carbon cycle operated in a fashion very different from younger times in Earth history. In this study, we offer new high-resolution data and a set of fresh constraints on the state and operation of the Late Archean carbon cycle, based on analyses of carbonate and organic carbon isotope ratios along a depth transect across the Campbellrand carbonate platform. This approach was guided by several specific questions: Did a large (~6‰) $\delta^{13}C$ gradient exist in the ocean basin in which the Campbellrand Platform precipitated? If not, then what accounts for the ^{13}C-depleted siderites from the associated iron formation? And finally, can we provide additional geologic context for the anomalously low $\delta^{13}C$ values commonly observed in Late Archean organic carbon?

Previous measurements of Late Archean stromatolitic carbonates yielded $\delta^{13}C$ values close to 0‰ (Schidlowski et al., 1975; Beukes et al., 1990; Veizer et al., 1992; Strauss and Moore, 1992; Shields and Veizer, 2002), and the new data from the Transvaal Supergroup agree with these observations. Furthermore, carbonates precipitated across a wide range of water depths in the Campbellrand-Kuruman sedimentary succession reveal approximately the same carbon isotope ratio (−0.5‰), establishing that the $\delta^{13}C$ of water column DIC was largely uniform. This isotopic distribution differs from that of DIC in ocean basins today. Considered within the context of the mathematical model developed above, these data suggest that either Late Archean oceans contained a much larger pool of DIC (in the face of greater atmospheric CO_2 concentrations hypothesized to keep the oceans from freezing) or that the biological pump was much weaker than today. Probably both were true. If future studies can place independent limits on the strength of the Late Archean biological pump, then, in principle, it should be possible to determine a lower limit on the pH of this ancient ocean.

Several observations suggest that the low $\delta^{13}C$ values measured within iron formation carbonate minerals (i.e., siderite) resulted from diagenetic remineralization of organic matter within precursor sediments. Sedimentologic and petrographic textures indicate that the siderite microbands commonly found in Campbellrand and Kuruman iron formation were present in the sediments during early diagenesis, prior to sedimentary compaction (Beukes, 1984; Beukes et al., 1990; this study). The pattern of carbon isotope ratios in iron formation siderite bolsters this conclusion and provides support for existing ideas that envision microbial iron respiration as a key process linked to the deposition of Late Archean iron formation. It has been noted many times previously that sideritic iron formation is commonly ^{13}C-depleted, with values as low as −15‰ reported

(Becker and Clayton, 1972; Perry and Tan, 1972; Beukes et al., 1990; Kaufman et al., 1990; Kaufman, 1996; Ohmoto et al., 2004). Our data confirm this, but also indicate that some iron formation siderites had $\delta^{13}C$ values close to those of calcites and dolomites in shallower parts of the same basin. Given a water column where DIC is constrained to be around −0.5, this strongly suggests that the siderites were precipitated diagenetically from sedimentary pore fluids where organic matter remineralization was commonly strong enough to alter significantly the $\delta^{13}C$ of local DIC. In modern marine environments, the carbon isotopic composition of carbonates precipitated from within pore fluids can depart strongly from water column values (e.g. Irwin et al., 1977; Mazzullo, 2000).

The precipitation of siderite during diagenesis of organic-rich sediments can be described by the following reactions. Ferric hydroxides are reduced to soluble ferrous iron with electrons from organic matter (represented here by formaldehyde):

$$CH_2O + 8H^+ + 4Fe(OH)_3 \Rightarrow 4Fe^{2+}_{(aq)} + CO_2 + 11H_2O \quad (11)$$

This process acts as a strong alkalinity pump and will tend to drive the precipitation of siderite (which is rather insoluble compared with other carbonate salts; Stumm and Morgan, 1996):

$$Fe^{2+}_{(aq)} + CO_2 + H_2O \Rightarrow FeCO_3 + 2H^+ \quad (12)$$

The carbon isotope ratios of siderite will therefore carry some isotopic memory of the remineralized organic carbon. Additional support for an early diagenetic origin of the siderites is provided by the range and scale of variability demonstrated by siderite $\delta^{13}C$ values. We observe that siderite $\delta^{13}C$ values vary on a cm-scale from near water column values (−0.5‰ as determined by deep water precipitates) to <−7‰. A similar pattern of variation has been reported in iron formations from the Hamersley Supergroup of Western Australia (Baur et al., 1985). This length scale of variability again points to a pore fluid origin, where organic concentrations can be large relative to the DIC reservoir size, respiration is fast, and mixing is limited largely by the timescale of diffusion. Ultimately, the precipitation and isotopic composition of siderite suggests that similar fluxes of ferric hydroxides and organic matter were supplied to sediment-starved areas undergoing iron formation deposition. The consumption of organic matter coupled to iron reduction (reaction (11)) probably occurred rapidly (Lovely et al., 1991), altering the pore fluid carbon isotopic abundances. Thus, the variable and often ^{13}C-depleted isotopic composition of iron formation siderites, in contrast with the uniform carbon isotope abundances of deep water carbonate precipitates, provides support for hypotheses that implicate microbial iron respiration as a conspicuous metabolism in Late Archean sedimentary environments (e.g. Walker, 1984; Vargas et al., 1998; Johnson et al., 2003, 2004; Konhauser et al., 2005; Archer and Vance, 2006; Fischer and Knoll, 2009).

The relative abundance of carbon isotopes preserved in ancient organic matter records complex interactions among a variety of processes, from different biochemical mechanisms of fixing and remineralizing carbon to variations in paleoenvironmental chemistry and post-depositional diagenesis and metamorphism. Preferential loss of isotopically light (relative to the parent material), low molecular weight hydrocarbons during post-depositional thermal degradation results in a lower H/C ratio and a ^{13}C-enrichment of residual kerogen (McKirdy and Powell, 1974). Because dehydrogenation will tend to drive the $\delta^{13}C$ higher, it suggests that the anomalously light carbon isotope abundances measured from Late Archean successions (Strauss and Moore, 1992; Beukes et al., 1990; Strauss and Beukes, 1996; this study) might more closely describe the primary depositional organic carbon composition. Despite this, the required differences in H/C ratios [from primary H/C = 1.2 down to <0.1 (Eq. (3) from Des Marais et al., 1992)] are probably too great to account for the wide variability of values more positive than the minima present in GKP01 and GKF01 organic carbon $\delta^{13}C$ (Waldbauer et al., this volume). This suggests that either additional diagenetic processes affected organic carbon isotopic composition in addition to dehydrogenation, or that there was significant isotopic heterogeneity present within the ancient sedimentary environment. Our observed m-scale lithologic pattern, wherein shale organics tend to be more ^{13}C-depleted than carbonate organics, is also present in other organic $\delta^{13}C$ datasets from Late Archean strata (Strauss et al., 1992a; Strauss and Beukes, 1996; Eigenbrode and Freeman, 2006). Whether this pattern reflects true, albeit slight, paleoenvironmental differences (Eigenbrode and Freeman, 2006) or differing patterns of diagenesis is difficult to know with certainty. We note that areas in GKP01 and GKF01 that contain interbedded shale and carbonate horizons accumulated both organic matter and carbonate minerals in essentially the same paleoenvironments – there does not appear to be any clear trend with water depth between correlative sequences in the two cores. This is highlighted in GKP01, where markedly light carbon isotope ratios occur in shaly units of both shallow water facies in the lower part of the succession and deep water facies near the top (Fig. 8). When constrained by lithology, organic carbon in the intervening carbonate-rich interval shows no strong facies trend. Host lithology appears to be a good predictor of organic carbon isotopic composition, whereas paleoenvironment and water depth do not. The effects of diagenesis notwithstanding, it is difficult to find a unique biological interpretation of the organic carbon $\delta^{13}C$ data. If the pattern of carbon isotope fractionation exhibited by extant biochemistry (Hayes, 2001) was present unchanged in the Late Archean (a somewhat tenuous assumption) then the data documented herein are consistent with several different mechanisms of carbon fixation, including secondary modification by heterotrophic processes. In particular, the presence of values <−40‰ may reflect abundant ecosystem methanotrophy (Schoell and Wellmer, 1981; Hayes, 1994; Hinrichs, 2002), although as yet it is difficult to rule out additional processes, such as autotrophic carbon fixation by carbon monoxide dehydrogenase via the reductive acetyl CoA pathway (Hayes, 2001). What global datasets make clear is that comparably ^{13}C-depleted organic matter occurs more often in Late Archean rocks than in younger successions (Strauss et al., 1992a; Strauss and Moore, 1992; Shields and Veizer, 2002; Eigenbrode and Freeman, 2006).

To the degree that the rock sequences studied here capture global biogeochemical conditions, our results provide valuable insight into the burial history of organic matter and the interaction between acid–base and redox facets of the Late Archean carbon cycle. If the $\delta^{13}C$ of DIC was uniform or nearly so in Late Archean oceans, the isotopic composition of basalt carbonates would have mirrored seawater. This is supported in part by carbon isotope measurements from carbonates within Archean seafloor basalts ($\delta^{13}C = -0.3$‰, Nakamura and Kato, 2004). Put another way, the term Δ_s in equation (3) goes to zero and the method for estimating organic carbon burial derived by Bjerrum and Canfield (2002) reverts to the standard model described by Eq. (1). If correct, this confirms that the burial of organic carbon was significant (steady-state estimates from our data suggest $f_{org} \approx .15$) and necessitates a flux of oxidants into the fluid Earth at this time. If water was the primary source of electrons for Late Archean autotrophs then a flux of O_2 into the environment must have existed prior to the rise of atmospheric oxygen (Kump et al., 2001; Holland, 2002). However, if Fe(II) was the primary electron donor, iron formation oxide minerals might account for the required oxidant flux (Walker, 1987; Widdel et al., 1993; Konhauser et al., 2002).

The relative stability of f_{org} through both anoxic and oxic epochs of Earth history is remarkable. Mechanisms that control organic carbon burial have been suggested to provide feedbacks that stabilize the oxygen content of the atmosphere; these proposals rely

either directly (Hedges and Keil, 1995; Hartnett et al., 1998) or indirectly (VanCappellen and Ingall, 1996; Colman and Holland, 2000) on environmental O_2 levels. What feedback(s) controlled the burial of organic carbon during Archean time, before the rise of oxygen? Data such as those from the Campbellrand–Kuruman sedimentary succession raise the possibility that a mechanism exists, as yet unrecognized, that controls the burial fractions of carbonate and organic matter over long time scales, both in the presence and absence of environmental oxygen.

Acknowledgements

The authors wish to acknowledge Jake Waldbauer and Jay Kaufman for reviews. We thank John Higgins, Paul Hoffman, and Ann Pearson for helpful discussions. WWF and AHK thank the Agouron Institute for funding. Half cores of GKP01, GKF01, and BH1-Sacha are currently housed at the Council for Geoscience in Tshwane (formerly Pretoria), Gauteng Province, South Africa. The cores GKP01 and GKF01 were collected as part of the Agouron Drilling Project (http://agouron.spectraconsulting.co.za).

References

Adams, E.W., Schlager, W., 2000. Basic types of submarine slope curvature. Journal of Sedimentary Research 70, 814–828.
Alt, J.C., Teagle, D.A.H., 1999. The uptake of carbon during alteration of ocean crust. Geochimica et Cosmochimica Acta 63, 1527–1535.
Altermann, W., Nelson, D.R., 1998. Sedimentation rates, basin analysis and regional correlations of three Neoarchean and Paleoproterozoic sub-basins of the Kaapvaal Craton as inferred from precise U-Pb zircon ages from volcani-clastic sediments. Sedimentary Geology 120, 225–256.
Altermann, W., Siegfried, H.P., 1997. Sedimentology and facies development of an Archean shelf: carbonate platform transition in the Kaapvaal Craton, as deduced from a deep borehole at Kathu, South Africa. Journal of African Earth Sciences 24, 391–410.
Archer, C., Vance, D., 2006. Coupled Fe and S isotope evidence for Archean microbial Fe(III) and sulfate reduction. Geology 34, 153–156.
Armstrong, R.A., Compston, W., Retief, E.A., Williams, I.S., Welke, H.J., 1991. Zircon ion microprobe studies bearing on the age and evolution of the Witwatersrand triad. Precambrian Research 53, 243–266.
Barton, E.S., Altermann, W., Williams, I.S., Smith, C.B., 1994. U-Pb zircon age for a tuff in the Campbell Group, Griqualand West Sequence, South Africa: implication for Early Proterozoic rock accumulation rates. Geology 22, pp. 343–246.
Barton Jr., J.M., Blignaut, E., Salnikova, E.B., Kotov, A.B., 1995. The stratigraphic position of the Buffelsfontein Group based on field relationships and geochemical and geochronological data. South African Journal of Geology 98, 386–392.
Baur, M.E., Hayes, J.M., Studley, S.A., Walter, M.R., 1985. Millimeter-scale variations of stable isotope abundances in carbonates from banded iron-formations in the Hamersley Group of Western Australia. Economic Geology 80, 270–282.
Becker, R.H., Clayton, R.N., 1972. Carbon isotopic evidence for the origin of a banded iron-formation in Western Australia. Geochimica et Cosmochimica Acta 36, 577–595.
Bekker, A., Holland, H.D., Wang, P.L., Rumble, D., Stein, H.J., Hannah, J.L., Coetzee, L.L., Beukes, N.J., 2004. Dating the rise of atmospheric oxygen. Nature 427, 117–120.
Beukes, N.J., Klein, C., Kaufman, A.J., Hayes, J.M., 1990. Carbonate petrography, kerogen distribution, and carbon and oxygen isotope variations in and early Proterozoic transition from limestone to iron formation deposition: Transvaal Supergroup, South Africa. Economic Geology 85, 663–690.
Beukes, N.J., 1987. Facies relations, depositional environments and diagenesis in a major early Proterozoic stromatolitic carbonate platform to basinal sequence, Campbellrand Supgroup, Transvaal Supergroup, southern Africa. Sedimentary Geology 54, 1–46.
Beukes, N.J., Smit, C.A., 1987. New evidence for thrusting in Griqualand West, South Africa: implications for stratigraphy and the age of red beds. South African Journal of Geology 90, 378–394.
Beukes, N.J., 1984. Sedimentology of the Kuruman and Griquatown iron-formations, Transvaal Supergroup, Griqualand West, South Africa. Precambrian Research 24, 47–84.
Bjerrum, C.J., Canfield, D.E., 2004. New insights into the burial history of organic carbon on the early Earth. Geochemistry Geophysics Geosystems G^3, 2004GC000713.
Bjerrum, C.J., Canfield, D.E., 2002. Ocean productivity before about 1.9 Gyr ago limited by phosphorus adsorption onto iron oxides. Nature 417, 159–162.
Brocks, J.J., Buick, R., Logan, G.A., Summons, R.E., 2003a. Composition and syngeneity of molecular fossils from the 2.78–2.45 billion-year-old Mount Bruce Supergroup, Pilbara Craton, Western Australia. Geochemica et Cosmochemica Acta 67, 4289–4319.
Brocks, J.J., Buick, R., Summons, R.E., Logan, G.A., 2003b. A reconstruction of Archean biological diversity based on molecular fossils from the 2.78–2.45 billion-year-old Mount Bruce Supergroup, Hamersley Basin, Western Australia. Geochemica et Cosmochemica Acta 67, 4321–4335.
Broecker, W.S., Peng, T.H., 1982. Tracers in the Sea. Lamont-Doherty Geological Observatory, Palisades, NY, p. 690.
Button, A., 1973. The stratigraphic history of the Malmani dolomite in the eastern and north-eastern Transvaal. Geological Society of South Africa Transactions 76, 229–247.
Canfield, D.E., Rosing, M.T., Bjerrum, C., 2006. Early anaerobic metabolisms. Philosophical Transactions of the Royal Society Series B 361, 1819–1836.
Canfield, D.E., 2005. The early history of atmospheric oxygen: homage to Robert M. Garrels. Annual Reviews of Earth and Planetary Sciences 33, 1–36.
Colman, A.S., Holland, H.D, 2000. The global diagenetic flux of phosphorus from marine sediments to the oceans: redox sensitivity and the control of atmospheric oxygen levels. Marine Authigenesis: From Global to Microbial. SEPM Special Publication No. 66.
Des Marais, D.J., Strauss, H., Summons, R.E., Hayes, J.M., 1992. Carbon isotopic evidence for the stepwise oxidation of the Proterozoic environment. Nature 359, 605–609.
Ebelmen, J.J., 1845. Sur les produits de la décomposition des especes minerals de la famille des silicates. Annales des Mines 7, 3–66.
Eigenbrode, J.L., Freeman, K.H., 2006. Late Archean rise of aerobic microbial ecosystems. Proceedings of the National Academy of Sciences USA 103, 15759–15764.
Farquhar, G.D., Ehleringer, J.R., 1989. Carbon isotopic discrimination and photosynthesis. Annual Reviews of Plant Physiology and Plant Molecular Biology 40, 503–537.
Farquhar, J., Bao, H.M., Thiemens, M., 2000. Atmospheric influence of Earth's earliest sulfur cycle. Science 289, 756–758.
Fischer, W.W., Knoll, A.H., 2009. An iron shuttle for deepwater silica in Late Archean and early Paleoproterozoic iron formation. Geological Society of America Bulletin 121, 222–235.
Grotzinger, J.P., Kasting, J.F., 1993. New constraints on Precambrian ocean composition. The Journal of Geology 101, 235–243.
Hartnett, H.E., Keil, R.G., Hedges, J.I., Devol, A.H., 1998. Influence of oxygen exposure time on organic carbon preservation in continental margin sediments. Nature 391, 572–574.
Hayes, J.M., Waldbauer, J.R., 2006. The carbon cycle and associated redox processes through time. Philosophical Transactions of the Royal Society B: Biological Sciences 361, 931–950.
Hayes, J.M., 2001. Fractionation of the isotopes of carbon and hydrogen in biosynthetic processes. Reviews in Mineralogy and Geochemistry 43, 225–278.
Hayes, J.M., 1994. Global methanotrophy at the Archean-Proterozoic transition. In: Bengston, S. (Ed.), Early Life on Earth, vol. 84. Columbia University Press, New York, pp. 200–236 (Nobel Symposium).
Hedges, J.I., Keil, R.G., 1995. Sedimentary organic matter preservation: an assessment and speculative synthesis. Marine Chemistry 49, 81–115.
Hinrichs, K.U., 2002. Microbial fixation of methane carbon at 2.7 Ga: was an anaerobic mechanism possible? Geochemistry Geophysics Geosystems 3, 2001GC000286.
Holland, H.D., 1972. The geologic history of sea water-an attempt to solve the problem. Geochimica et Cosmochimica Acta 36, 637–651.
Holland, H.D., 2002. Volcanic gases, black smokers, and the great oxidation event. Geochimica et Cosmochimica Acta 66, 3811–3826.
Hotinski, R.M., Kump, L.R., Arthur, M.A., 2004. The effectiveness of the Paleoproterozoic biological pump: d13C gradients from platform carbonates of the Pethei Group (Great Slave Lake Supergroup, N.W.T.). Bulletin of the Geological Society of America 116, 539–554.
Hut, G., 1987. Consultant's group meeting on stable isotope reference samples for geochemical and hydrological investigations. IAEA report, Vienna, September 1985, 1–42.
Irwin, H., Curtis, C., Coleman, M., 1977. Isotopic evidence for source of diagenetic carbonates formed during burial of organic-rich sediments. Nature 269,209–213.
Jahnke, R.A., 1996. The global ocean flux of particulate organic carbon: Areal distribution and magnitude. Global Biogeochemical Cycles 1, 71–88.
Johnson, C.M., Beard, B.L., Newman, D.K., Nealson, K.H., 2004. Isotopic constraints on biogeochemical cycling of Fe. Reviews in Mineralogy and Geochemistry 55, 359–408.
Johnson, C.M., Beard, B.L., Beukes, N.J., Klein, C., O'Leary, J.M., 2003. Ancient geochemical cycling in the Earth as inferred from Fe isotope studies of banded iron formations from the Transvaal Craton. Contributions to Mineralogy and Petrology 144, 523–547.
Kasting, J.F., 1987. Theoretical constraints on oxygen and carbon dioxide concentrations in the Precambrian atmosphere. Precambrian Research 34, 205–229.
Kasting, J.F., 1993. Earth's early atmosphere. Science 259, 920–925.
Kaufman, A.J., 1996. Geochemical and mineralogic effects of contact metamorphism on banded iron-formation: an example from the Transvaal Basin, South Africa. Precambrian Research 79, 171–194.
Kaufman, A.J., Hayes, J.M., Klein, C., 1990. Primary and diagenetic controls of isotopic compositions of iron-formation carbonates. Geochimica et Cosmochimica Acta 54, 3461–3473.
Kharecha, P., Kasting, J., Siefert, J., 2005. A coupled atmosphere-ecosystem model of the early Archean Earth. Geobiology 3, 53–76.
Klein, C., Beukes, N.J., Schopf, J.W., 1987. Filamentous microfossils in the Early Proterozoic Transvaal Supergroup: their morphology, significance, and paleoenvironmental setting. Precambrian Research 36, 81–84.
Konhauser, K.O., Newman, D.K., Kappler, A., 2005. The potential significance of microbial Fe(III) reduction during deposition of Precambrian banded iron formations. Geobiology 3, 167–177.

Konhauser, K.O., Hamade, T., Raiswell, R., Morris, R.C., Ferris, F.G., Southam, G., Canfield, D.E., 2002. Could bacteria have formed the Precambrian banded iron formations? 30, 1079–1082.
Kroopnik, P., 1980. The distribution of ^{13}C in the Atlantic Ocean. Earth and Planetary Science Letters 30, 469–484.
Kump, L.R., 1991. Interpreting carbon-isotope excursions: Strangelove oceans. Geology 19, 299–302.
Kump, L.R., Kasting, J.F., Barley, M.E., 2001. Rise of atmospheric oxygen and the "upside-down" Archean mantle. Geochemistry Geophysics Geosystems G^3, 2000GC000114.
Lovely, D.R., Phillips, E.J.P., Lonergan, D.J., 1991. Enzymatic versus nonenzymatic mechanisms for Fe(III) reduction in aquatic sediments. Environmental Science and Technology 25, 1062–1067.
Mazzullo, S.J., 2000. Organogenic dolomitization in peritidal to deep-sea sediments. Journal of Sedimentary Research 70, 10–23.
McCave, I.N., 1975. Vertical flux of particles in the ocean. Deep-Sea Research 22, 491–502.
McKirdy, D.M., Powell, T.G., 1974. Metamorphic alteration of carbon isotopic composition of ancient sedimentary organic matter: new evidence from Australia and South Africa. Geology 2, 591–595.
McCrea, J.M., 1950. On the isotopic chemistry of carbonates and a paleotemperature scale. Journal of Chemical Physics 18, 849–857.
Miyano, T., Beukes, N.J., 1984. Phase relations of stilpnomelane, ferriannite, and riebekite in very low-grade metamorphosed iron formations. Geological Society of South Africa Transactions 87, 111–124.
Nakamura, K., Kato, Y., 2004. Carbonatization of oceanic crust by the seafloor hydrothermal activity and its significance as a CO_2 sink in the Early Archean. Geochimica et Cosmochimica Acta 68, 4595–4618.
Nier, A.O., Gulbrandsen, E.A., 1939. Variations in the relative abundances of the carbon isotopes. Journal of the American Chemical Society 61, 697–699.
Ohmoto, H., Watanabe, Y., Kumazawa, K., 2004. Evidence from massive siderite beds for a CO_2-rich atmosphere before approximately 1.8 billion years ago. Nature 429, 395–399.
Owen, T., Cess, R.D., Ramanathan, V., 1979. Enhanced CO_2 greenhouse to compensate for reduced solar luminosity on early Earth. Nature 277, 640–642.
Pavlov, A.A., Kasting, J.F., 2002. Mass-independent fractionation of sulfur isotopes in Archean sediments: strong evidence for an anoxic Archean atmosphere. Astrobiology 2, 27–41.
Perry Jr., E.C., Tan, F.C., 1972. Significance of oxygen and carbon isotope variations in early Precambrian cherts and carbonate rocks of Southern Africa. Geological Society of America Bulletin 83, 647–664.
Pickard, A.L., 2003. SHRIMP U-Pb zircon ages for the Paleoproterozoic Kuruman Iron Formation, Northern Cape Province, South Africa: evidence for simultaneous BIF deposition on Kaapvaal and Pilbara Cratons. Precambrian Research 125, 275–315.
Rasmussen, B., Buick, R., 1999. Redox state of the Archean atmosphere: evidence from detrital heavy minerals in ca. 3250–2750 Ma sandstones from the Pilbara Craton, Australia. Geology 27, 115–118.
Rye, R., Holland, H.D., 1998. Paleosols and the evolution of atmospheric oxygen: a critical review. American Journal of Science 298, 621–672.
Sagan, C., Mullen, S., 1972. Earth and Mars: evolution of atmospheres and surface temperatures. Science 177, 52–56.
Schidlowski, M., Eichmann, R., Junge, C.E., 1975. Precambrian sedimentary carbonates: carbon and oxygen isotope geochemistry and implications for the terrestrial oxygen budget. Precambrian Research 2, 1–69.
Schmitz, M.D., Bowring, S.A., 2003. Ultrahigh-temperature metamorphism in the lower crust during Neoarchean Ventersdorp rifting and magmatism, Kaapvaal Craton, southern Africa. Bulletin of the Geological Society of America 115, 533–548.
Schoell, M., Wellmer, F.-W., 1981. Anomalous ^{13}C depletion in early Precambrian graphites from Superior Province, Canada. Nature 290, 696–699.
Schröder, S., Lacassie, J.P., Beukes, N.J., 2006. Stratigraphic and geochemical framework of the Agouron drill cores, Transvaal Supergroup (Neoarchean-Paleoproterozoic, South Africa). South African Journal of Geology 109, 23–54.
Scott, K.M., Schwedock, J., Schrag, D.P., Cavanaugh, C.M., 2004. Influence of form 1A RubisCO and environmental dissolved inorganic carbon on the $\delta^{13}C$ of the clam-chemoautotroph symbiosis *Solemya velum*. Environmental Microbiology 6, 1210–1219.
Shields, G., Veizer, J., 2002. Precambrian marine carbonate isotope database: Version 1.1. Geochemistry Geophysics Geosystems G^3, 2001GC000266.
Sleep, N.H., Zahnle, K., 2001. Carbon dioxide cycling and implications for climate. Journal of Geophysical Research 106, 1373–1399.
Smayda, T.J., 1970. The suspension and sinking of phytoplankton in the sea. Oceanography and Marine Biology Annual Review 8, 353–414.
Staudigel, H., Hart, S.R., Schmincke, H.U., Smith, B.M., 1989. Cretaceous ocean crust at DSDP Sites 417 and 418: Carbon uptake from weathering versus loss by magmatic outgassing. Geochimica et Cosmochimica Acta 53, 3091–3094.
Stowe, C.W., 1986. Synthesis and interpretation of structures along the northeastern boundary of the Namaqua tectonic province, South Africa. Geological Society of South Africa Transactions 89, 185–198.
Strauss, H., Des Marais, D.J., Hayes, J.M., Summons, R.E., 1992a. The carbon-isotopic record. In: Schopf, J.W., Klein, C. (Eds.), The Proterozoic Biosphere: A Multidisciplinary Study. Cambridge University Press, Cambridge, pp. 117–127.
Strauss, H., Des Marais, D.J., Hayes, J.M., Summons, R.E., 1992b. Procedures of whole rock and kerogen analysis. In: Schopf, J.W., Klein, C. (Eds.), The Proterozoic Biosphere. Cambridge University Press, pp. 701–702.
Strauss, H., Moore, T.B., 1992. Abundances and isotopic compositions of carbon and sulfur species in whole rock and kerogen samples. In: Schopf, J.W., Klein, C. (Eds.), The Proterozoic Biosphere: A Multidisciplinary Study. Cambridge University Press, Cambridge, pp. 709–798.
Strauss, H., Beukes, N.J., 1996. Carbon and sulfur isotopic compositions of organic carbon and pyrite in sediments from the Transvaal Supergroup, South Africa. Precambrian Research 79, 57–71.
Stumm, W., Morgan, J.J., 1996. Aquatic Chemistry, 3rd edition. John Wiley & Sons, New York, p. 1022.
Sumner, D.Y., Beukes, N.J., 2006. Sequence stratigraphic development of the Neoarchean Transvaal carbonate platform, Kaapvaal Craton, South Africa. South African Journal of Geology 109, 11–22.
Sumner, D.Y., Grotzinger, J.P., 2000. Evidence for Late Archean aragonite precipitation: petrography, facies associations, and environmental significance. In: Grotzinger, J., James, N. (Eds.), Carbonate Sedimentation and Diagenesis in the Evolving Precambrian World. SEPM Special Publication, pp. 123–144.
Sumner, D.Y., Grotzinger, J.P., 2004. Implications for Neoarchean ocean chemistry from primary carbonate mineralogy of the Campbellrand-Malmani Platform, South Africa. Sedimentology 51, 1–27.
Sumner, D.Y., 1997a. Carbonate precipitation and oxygen stratification in Late Archean seawater as deduced from facies and stratigraphy of the Gamohaan and Frisco Formations, Transvaal Supergroup, South Africa. American Journal of Science 297, 455–487.
Sumner, D.Y., 1997b. Late Archean calcite-microbe interactions: two morphologically distinct microbial communities that affected calcite nucleation differently. Palaios 12, 302–318.
Sumner, D.Y., Grotzinger, J.P., 1996a. Were kinetics of Archean calcium carbonate precipitation related to oxygen concentration? Geology 24, 119–122.
Sumner, D.Y., Grotzinger, J.P., 1996b. Herringbone calcite: petrography and environmental significance. Journal of Sedimentary Research 66, 419–429.
Sumner, D.Y., Bowring, S.A., 1996. U-Pb geochronologic constraints on deposition of the Campbellrand Subgroup, Transvaal Supergroup, South Africa. Precambrian Research 78, 25–35.
Sumner, D.Y., 1995. Facies, paleogeography, and carbonate precipitation on the Archean (2520 Ma) Campbellrand–Malmani Platform, Transvaal Supergroup, South Africa. PhD Thesis, Massachusetts Institute of Technology, p. 514.
Sundquist, E., 1985. Geological perspectives on carbon dioxide and the carbon cycle. In: Sundquist, E., Broecker, W. (Eds.), The Carbon Cycle and Atmospheric CO2: Natural Variations Archean to Present. AGU, Washington.
Turner, J.T., 2002. Zooplankton fecal pellets, marine snow and sinking phytoplankton blooms. Aquatic Microbial Ecology 27, 57–102.
Urey, H.C., 1947. The thermodynamic properties of isotopic substances. Journal of the Chemical Society, 562–581.
VanCappellen, P., Ingall, E.D., 1996. Redox stabilization of the atmosphere and oceans by phosphorus-limited marine productivity. Science 271, 493–496.
Vargas, M., Kashefi, K., Blunt-Harris, E.L., Lovley, D.R., 1998. Microbiological evidence for Fe(III) reduction on early Earth. Nature 395, 65–67.
Veizer, J., Clayton, R.N., Hinton, R.W., 1992. Geochemistry of Precambrian carbonates. IV. Early Paleoproterozoic (2.25 ± 0.25 Ga) seawater. Geochimica et Cosmochimica Acta 56, 875–885.
Waldbauer, J., et al., this volume. Late Archean molecular fossils from the Transvaal Supergroup record the antiquity of microbial diversity and aerobiosis. Precambrian Research.
Walker, J.C.G., Hays, P.B., Kasting, J.F., 1981. A negative feedback mechanism for the long-term stabilization of Earth's surface temperature. Journal of Geophysical Research 86, 9776–9782.
Walker, J.C.G., 1983. Possible limits on the composition of the Archean ocean. Nature 302, 518–520.
Walker, J.C.G., 1984. Suboxic diagenesis in banded iron formations. Nature 309, 340–342.
Walker, J.C.G., 1987. Was the Archean biosphere upside down? Nature 329, 710–712.
Walker, J.C.G., 1990. Precambrian evolution of the climate system. Global and Planetary Change 82, 261–289.
Walraven, F., Martini, J., 1995. Zircon Pb-evaporation age determinations of the Oak Tree Formation, Chuniespoort Group, Transvaal Sequence: implications for the Transvaal-Griqualand West basin correlations. South African Journal of Geology 98, 58–67.
Wickman, F.E., 1956. The cycle of carbon and the stable carbon isotopes. Geochimica et Cosmochimica Acta 9, 136–153.
Widdel, F., Schnell, S., Heising, S., Ehrenreich, A., Assmus, B., Schink, B., 1993. Ferrous iron oxidation by anoxygenic phototrophic bacteria. Nature 362, 834–836.
Wing, B.A., Brabson, E., Farquhar, J., Kaufman, A.J., Rumble, D., Bekker, A., 2002. D33S, d34S and d13C constraints on the Paleoproterozoic atmosphere during the earliest Huronian glaciation. In: Proceedings of the 12th Goldschmidt Conference, p. A840.
Winter, B.L., Knauth, L.P., 1992. Stable isotope geochemistry of cherts and carbonates from the 2.0 Ga Gunflint Iron Formation: implications for the depositional setting, and the effects of diagenesis and metamorphism. Precambrian Research 59, 283–314.
Zeebe, R.E., Wolf-Gladrow, D., 2001. CO_2 in Seawater: Equilibrium, Kinetics, Isotopes. Elsevier, Boston, p. 346.